ELSEVIER

Applied Surface Science 190 (2002) 121–128

applied surface science

www.elsevier.com/locate/apsusc

# Core-level photoemission of the Si(1 1 1)–$\sqrt{21} \times \sqrt{21}$-Ag surface using synchrotron radiation

Xiao Tong[a], Satoru Ohuchi[b], Takehiro Tanikawa[b], Ayumi Harasawa[c], Taichi Okuda[c], Yoshinobu Aoyagi[a], Toyohiko Kinoshita[c], Shuji Hasegawa[b,*]

[a]*The Institute of Physical and Chemical Research (RIKEN), Hirosawa, Wako-shi, Saitama 351-0198, Japan*
[b]*Department of Physics, School of Science, University of Tokyo, 7-3-1 Hongo, Bunkyo-ku, Tokyo 113-0033, Japan*
[c]*Synchrotron Radiation Laboratory, The Institute of Solid State Physics, University of Tokyo, 5-1-5 Kashiwanoha, Kashiwa, Chiba 277-8581, Japan*

**Abstract**

The evolution of Si 2p core-level photoemission during a structural conversion from the Si (1 1 1)–$\sqrt{3} \times \sqrt{3}$-Ag to the Si(1 1 1)–$\sqrt{21} \times \sqrt{21}$-Ag superstructures induced by Ag adatoms adsorption at 140 K was studied using synchrotron radiation. The component from the top-layer Si-trimer atoms on the former surface was found to split into two components in the latter surface. The result is discussed in terms of a relaxation in some of the Si trimers induced by Ag adatoms sitting on the nearby Ag triangles of the $\sqrt{3} \times \sqrt{3}$-Ag substrate. The intensity ratio between the split components is a key to exclude some structure models proposed so far for the $\sqrt{21} \times \sqrt{21}$ phases. 

*Keywords:* Photoemission spectroscopy; Silicon; Silver

## 1. Introduction

The $\sqrt{21} \times \sqrt{21}$ superstructures are commonly formed by adsorption of sub-monolayer adatoms of noble metals (Au, Ag or Cu) [1–6] as well as alkali metals (Cs, K) [7,8] onto the Si(1 1 1)–$\sqrt{3} \times \sqrt{3}$-Ag surface, at room temperature (RT) or lower temperatures depending on the adatom species. Several techniques including scanning tunneling microscopy (STM) [1,2,6], reflection high-energy electron diffraction (RHEED) [3,5,9], angle-resolved photoemission spectroscopy (ARPES) [10,11], surface conductance measurements [5,12,13], together with theoretical efforts [14], have been devoted to study these surface phases. Then, some interesting common features in atomic/electronic structures and electrical transport properties were found [8]. However, fundamental questions such as adatom coverage required for these phases and their adsorption sites still remain.

In this paper, we present the evolution of Si 2p core-level photoemissions using synchrotron radiation during the structural conversion from the $\sqrt{3} \times \sqrt{3}$-Ag surface to the $\sqrt{21} \times \sqrt{21}$-Ag surface induced by Ag adatoms adsorption at 140 K. Core-level spectra constitute a very sensitive, yet indirect, probe of the atomic local structures; if measured with high resolution, surface core-level shifts from the substrate bulk atoms can provide useful information about atomic sites. The component from the top-layer Si-trimer atoms of the $\sqrt{3} \times \sqrt{3}$-Ag surface was found to split into two components on the $\sqrt{21} \times \sqrt{21}$-Ag surface. From the energy shifts and intensity ratio of the two components, some of the models proposed so far for

* Corresponding author. Tel./fax: +81-3-5841-4167.
*E-mail address*: shuji@surface.phys.s.u-tokyo.ac.jp (S. Hasegawa).

0169-4332/02/$ – see front matter 
PII: S0169-4332(01)00854-6

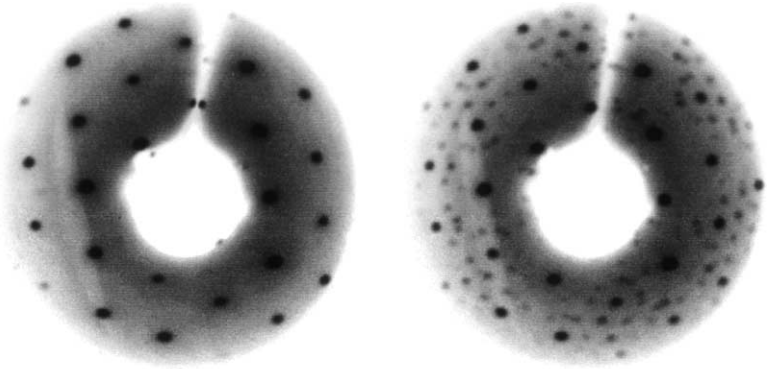


Fig. 1. LEED patterns at 140 K of: (a) Si(1 1 1)–$\sqrt{3} \times \sqrt{3}$-Ag surface, and (b) Si(1 1 1)–$\sqrt{21} \times \sqrt{21}$-Ag surface obtained by deposition of about 0.17 ML of Ag adatoms onto the $\sqrt{3} \times \sqrt{3}$-Ag surface, respectively.

the $\sqrt{21} \times \sqrt{21}$ phases are excluded. Taking the theoretical results into account [14], none of the proposed models are found to satisfy the structural features required for this surface.

## 2. Experimental

The synchrotron photoemission experiments were performed on a vacuum ultraviolet beam line BL-18A at Photon Factory of KEK, Tsukuba, Japan. The spectra were obtained with an angle-integrated-type hemispherical analyzer (VG-CLAM 2), and the photon irradiated the surface at 45° off the surface normal. The emission angle was selected to be 0° and 60° from the surface normal. Linearly polarized synchrotron radiation was used at energy of 132 eV for surface-sensitive mode and 108 eV for bulk-sensitive mode. The energy resolution of this system was about 80 meV.

The substrate was a p-type Si(1 1 1) wafer of 8–15 Ω cm resistivity at RT. A clear 7 × 7-LEED pattern was produced by flashing the sample at 1200 °C several times by direct current of about 10 A through it. The Si(1 1 1)–$\sqrt{3} \times \sqrt{3}$-Ag structure was made at a substrate temperature of 450 °C by depositing 1 ML of Ag atoms. After cooling the surface down to 140 K, the Si(1 1 1)–$\sqrt{21} \times \sqrt{21}$-Ag structure was formed by depositing Ag of 0.14–0.19 ML coverage onto the $\sqrt{3} \times \sqrt{3}$-Ag surface with a rate of 0.50 ML/min. The coverage and evaporation rate of Ag were calibrated by assuming that 1 ML of Ag was needed for complete conversions in LEED patterns from the 7 × 7 clean structure to the $\sqrt{3} \times \sqrt{3}$-Ag [15]. Fig. 1(a) shows a typical LEED pattern of the initial $\sqrt{3} \times \sqrt{3}$-Ag surface at 140 K, and Fig. 1(b) is that of the $\sqrt{21} \times \sqrt{21}$-Ag at 140 K. Sharp diffraction spots with low background mean good long-range orderings for both phases.

## 3. Results

Fig. 2(a) and (b) shows Si 2p core-level spectra taken with the surface-sensitive photon energy of 132 eV at normal emission from the initial $\sqrt{3} \times \sqrt{3}$-Ag and the $\sqrt{21} \times \sqrt{21}$-Ag surfaces, respectively. The overall shapes of the two spectra look quite different from each other, indicating different several components composing the peaks. Then the spectra were decomposed by using a standard method with the following fitting parameters: Gaussian width = 205 meV at full width at half maximum (FWHM), Lorentzian width = 83 meV (FWHM), spin-orbit splitting = 602 meV, and $p_{1/2}/p_{3/2}$ intensity branching ratio = 0.52. These parameters were determined by using the fitting results of bulk-sensitive spectra with photon energy of 108 eV. As shown in Fig. 2, the peak of the $\sqrt{3} \times \sqrt{3}$-Ag surface is decomposed into three components, two surface components $S_1$ and $S_2$, and a bulk one B. On one hand, the peak of the $\sqrt{21} \times \sqrt{21}$-Ag surface is composed of four components, three surface components P, Q and $S_2$, and a bulk one B. The

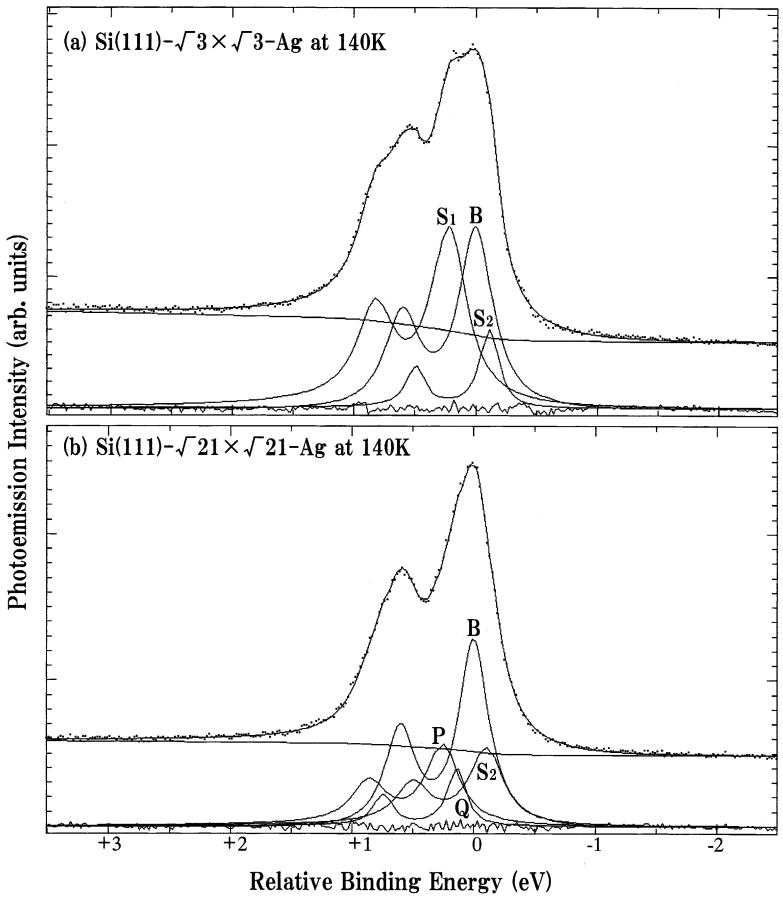


Fig. 2. Surface-sensitive Si 2p core-level spectra taken with a photon energy of 132 eV at normal emission from: (a) Si(1 1 1)–$\sqrt{3} \times \sqrt{3}$-Ag surface, and (b) Si(1 1 1)–$\sqrt{21} \times \sqrt{21}$-Ag surface, at 140 K, respectively. The relative binding energy scale is referred to the Si $2p_{3/2}$ line of the bulk component. The decomposed components are shown by the curves under the spectrum. Solid lines with data points show the fitting results.

asymmetry parameter $\alpha$ was set zero for B component, while $\alpha = 0.04$ for every surface components. We thus had to introduce the non-zero $\alpha$ to obtain good fittings, which means a metallic character of the surface. This feature is already reported by a previous study for the $\sqrt{3} \times \sqrt{3}$-Ag surface [16]. These decompositions were confirmed by the spectra taken at 60° emission angle, too. The details of the respective components are listed in Table 1.

Fig. 3 shows the Ag coverage dependence of the core-level shape measured at various coverages around 1 ML. The observed LEED patterns are indicated on the respective spectra. Below 1 ML coverages (Fig. 3(a) and (b)), the features in spectra are

Table 1
Energy shifts and intensities of the surface components with respect to the bulk one for the respective surface superstructures

| Surface | Components | Energy shifts (eV) | Relative intensity |
|---|---|---|---|
| $\sqrt{3} \times \sqrt{3}$-Ag | B | 0 | 0.41 |
| | $S_1$ | 0.22 | 0.41 |
| | $S_2$ | −0.12 | 0.18 |
| $\sqrt{21} \times \sqrt{21}$-Ag | B | 0 | 0.45 |
| | P | 0.25 | 0.20 |
| | Q | 0.14 | 0.15 |
| | $S_2$ | −0.11 | 0.20 |

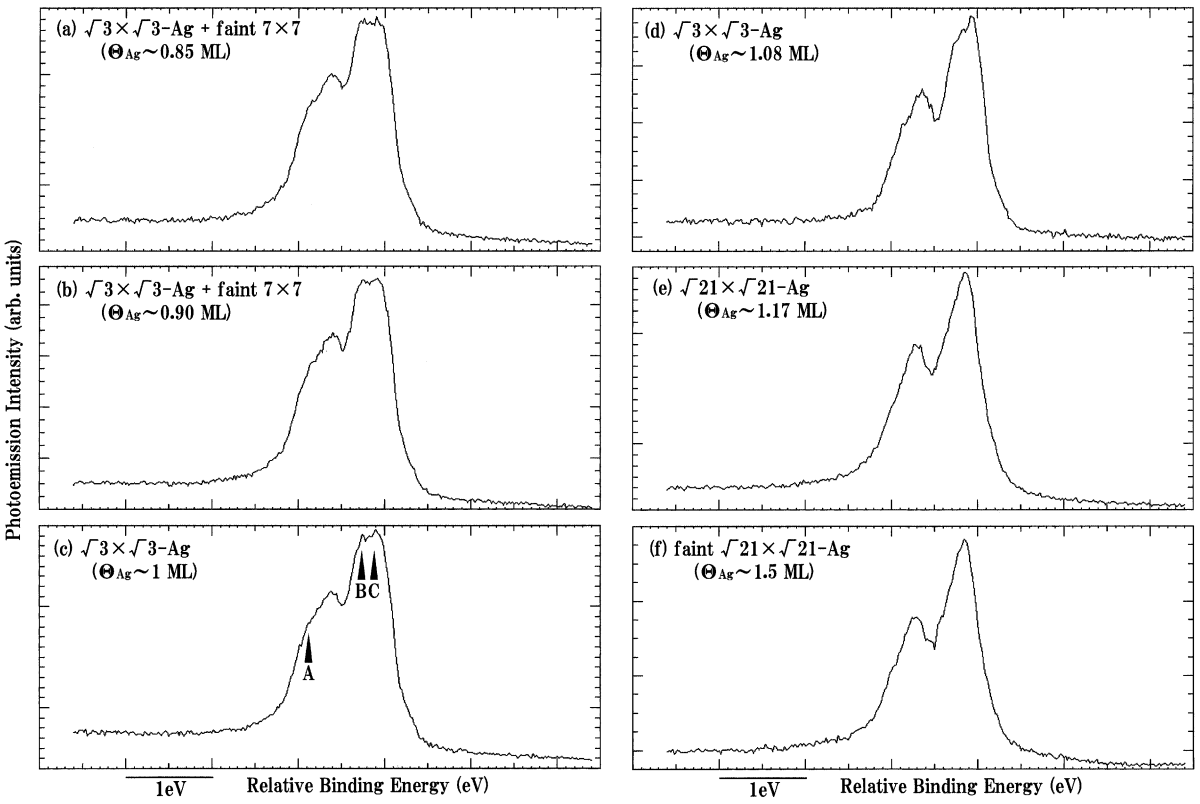


Fig. 3. Ag coverage $\Theta_{Ag}$ dependence of the Si 2p core-level spectra at 140 K.

similar to that of the $\sqrt{3} \times \sqrt{3}$-Ag phase (Fig. 3(c)). But once the coverage exceeds 1 ML (Fig. 3(d)), the shape seems to change into that of the $\sqrt{21} \times \sqrt{21}$-Ag phase (Fig. 3(e)); a shoulder A in Fig. 3(c) disappears, and double peaks B and C become a single peak in Fig. 3(e). The Ag adatoms over 1 ML coverage are known to be in 'two-dimensional adatom gas (2DAG)' phase [6,17] though the adatoms do not make any long-range orders. Around 0.17 ML coverage over 1 ML (Fig. 3(e)), the adatoms order in the $\sqrt{21}\times$ $\sqrt{21}$ periodicity on the $\sqrt{3} \times \sqrt{3}$-Ag substrate. Around 0.5 ML adatoms over 1 ML coverage (Fig. 3(f)), the adatoms begin to make clusters [6] where the $\sqrt{21} \times \sqrt{21}$-LEED spots fade, remaining the strong $\sqrt{3} \times \sqrt{3}$ spots. The core-level shape at this coverage looks similar to that of the $\sqrt{21} \times \sqrt{21}$ phase (Fig. 3(e)). In this way, the Si 2p core-level emission peak depends sensitively on the Ag coverage, especially the spectra look quite different between below and above 1 ML coverage, the saturation coverage for the $\sqrt{3} \times \sqrt{3}$-Ag structure.

## 4. Discussion

In the honeycomb-chained triangle (HCT) model for the $\sqrt{3} \times \sqrt{3}$-Ag structure [15], Si atoms in the top layer form trimers (gray circles in Fig. 4), each of which is bonded to an Ag atom (filled circles) by an ionic covalent bond. Three Ag atoms arrange in a triangle, and the triangles are connected to each other to make honeycomb chains. This is why this surface is called as HCT structure. In the previous studies of core-level spectroscopy of this surface [16,18], the $S_1$ component in Si 2p emission of Fig. 2(a) was assigned as an emission from the Si-trimer atoms, while the $S_2$ component come from the second Si layer bonded directly to the Si-trimer layer.

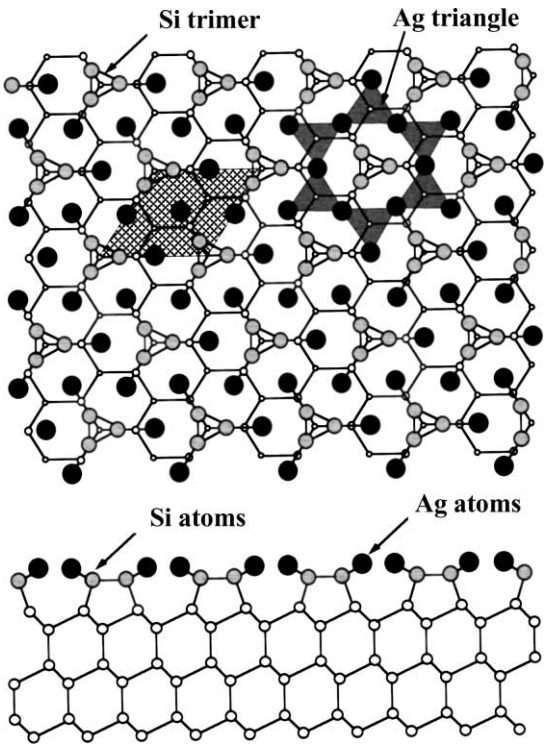


Fig. 4. Schematic representation of the atomic arrangement of Si(1 1 1)–$\sqrt{3} \times \sqrt{3}$-Ag surface superstructure, the so-called HCT model. Upper panel: plan view; lower panel: sectional view. A gray lozenge indicates the $\sqrt{3} \times \sqrt{3}$-unit cell, and gray triangles indicate 'Ag triangles'.

The fitting results for the $\sqrt{21} \times \sqrt{21}$-Ag surface (Fig. 2(b)) show that the $S_2$ component does not change so much compared to that of the $\sqrt{3} \times \sqrt{3}$-Ag structure (just slightly broadened). However, the $S_1$ component of the $\sqrt{3} \times \sqrt{3}$-Ag splits into two components, P and Q, which shift towards higher and lower binding energies by 0.03 and 0.08 eV compared to the initial $S_1$ position, respectively. This means that the equivalent Si-trimer atoms at the $\sqrt{3} \times \sqrt{3}$-Ag structure become inequivalent at the $\sqrt{21} \times \sqrt{21}$-Ag phase.

Before assigning the respective components of the $\sqrt{21} \times \sqrt{21}$-Ag spectra in Fig. 2(b), it is useful to address the structure models proposed so far for the $\sqrt{21} \times \sqrt{21}$ surfaces with Au or Ag adatoms adsorptions. Nogami et al. [1] proposed the adatoms sitting upon the center of some Ag triangles of the $\sqrt{3} \times \sqrt{3}$-Ag substrate (Fig. 5(a)). The adatom coverage is 0.24 ML in their model (five adatoms in the $\sqrt{21} \times \sqrt{21}$ unit cell). On the other hand, Ichimiya et al. [2] supposed the adatoms to be located above some of the Si trimers (Fig. 5(b)). The adatoms coverage is 0.14 ML in their model (three adatoms in the unit cell). Tong et al. [6] proposed a model in which the Ag adatoms sit on some of the Ag-triangle centers with the Ag adatom coverage of 0.19 ML (four adatoms in the unit cell) (Fig. 5(c)). All the models, however, suggest a common feature that the HCT framework of the initial $\sqrt{3} \times \sqrt{3}$-Ag substrate is not broken, rather just distorted with the adatoms adsorption in the $\sqrt{21} \times \sqrt{21}$ phases. Actually, the recent X-ray diffraction results show some distortion of the HCT framework, in which Tajiri et al. [19] proposed the other model for the $\sqrt{21} \times \sqrt{21}$ phase in which the unit cell contains five adatoms as Nogami's model (Fig. 5(d)). The Ag adatoms should sit on some of the center of Ag triangles in their model again, but the arrangement of adatoms is different from Nogami's model. In recent theoretical calculations in which Ag adatoms sit on the every Ag-triangle centers or every Si-trimer centers of the $\sqrt{3} \times \sqrt{3}$-Ag substrate to mimic the $\sqrt{21} \times \sqrt{21}$ structure [14], it has been found that the adatom energetically prefers to locate upon Ag triangles rather than upon Si trimers. So we here discuss our Si 2p spectra by using models in which Ag adatoms sit on some of the Ag triangles.

As mentioned before, each Si-trimer atom is bonded to an Ag atom that forms a triangle with other two Ag atoms (Fig. 4). All of the Si–Ag bonds therefore are equivalent in the $\sqrt{3} \times \sqrt{3}$-Ag phase. But once Ag adatoms adsorb on some of Ag triangle centers, the chemical environment at the Si–Ag bonds would be different depending on whether the Ag triangles have Ag adatoms on their center or not. Thus the top-layer Si atoms in the $\sqrt{21} \times \sqrt{21}$-Ag phase should have two different core levels. The P component (Fig. 2(b)) whose energy position is nearly the same as that of the initial $S_1$ component (Fig. 2(a)) could be associate to the top-layer Si atoms connected to the Ag-triangle atoms without Ag adatoms sitting on ('unaffected' Si atoms), while the Q component with a larger energy shift could be emission from the top-layer Si atoms connected to the Ag triangles with Ag adatoms sitting on them ('affected' Si atoms). This consideration is consistent with an RHEED rocking-curve analysis that the Si trimers are relaxed in the $\sqrt{21} \times \sqrt{21}$ phase [9]. Then we can count the numbers of top-layer Si atoms

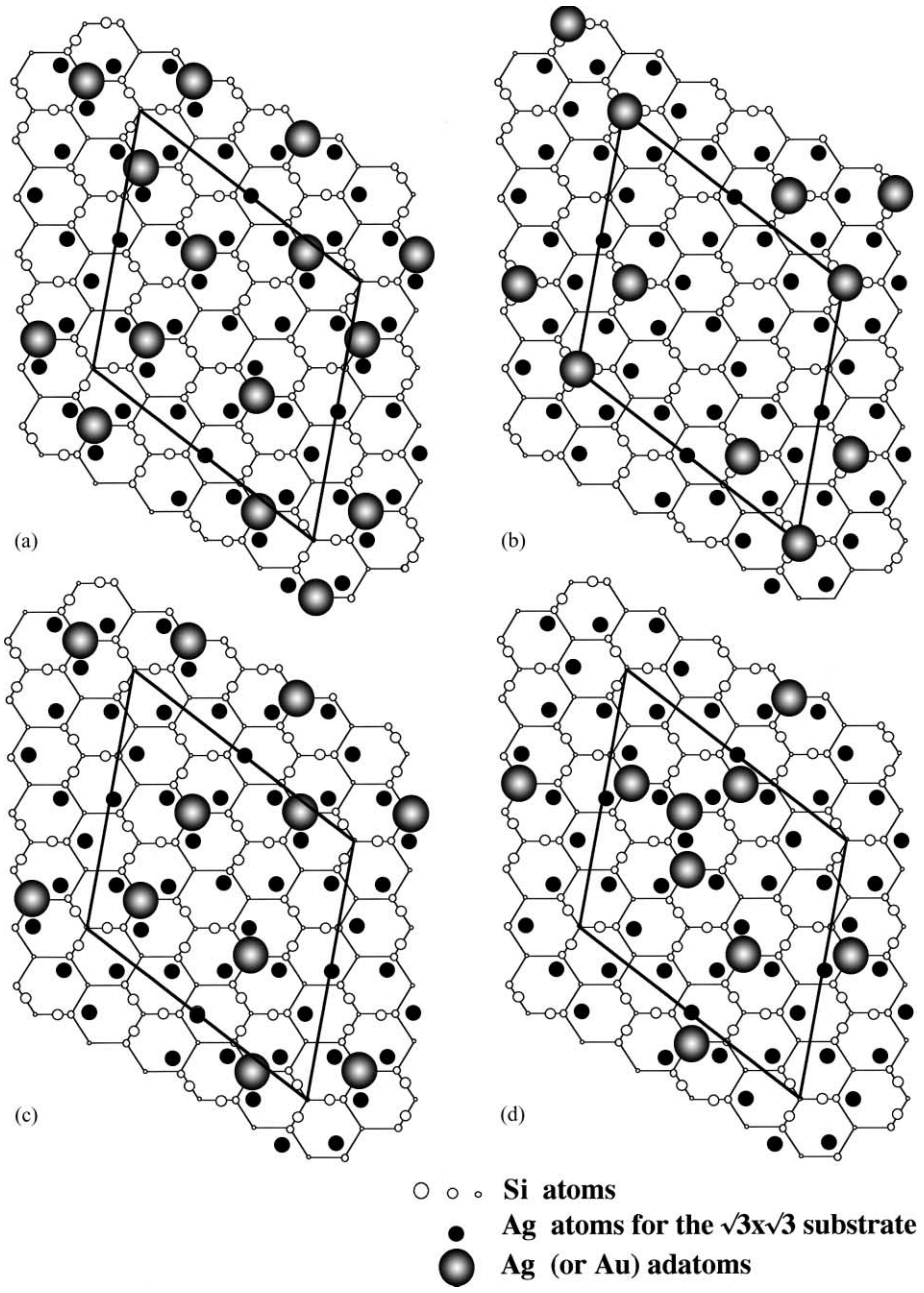


Fig. 5. Structural models proposed so far for the Si(1 1 1)-$\sqrt{21} \times \sqrt{21}$ surface superstructures induced by Ag or Au adatom adsorptions. (a) Nogami et al. [1]; (b) Ichimiya et al. [2]; (c) Tong et al. [5]; (d) Tajiri et al. [19]. A $\sqrt{21} \times \sqrt{21}$-unit cell is indicated by a lozenge.

corresponding to the P and Q components in the respective proposed models in Fig. 5, which are listed in Table 2, together with other features of the models.

ARPES for the valence bands [10,11] indicates that Ag or Au adatoms in the $\sqrt{21} \times \sqrt{21}$ surfaces donate their valence electrons into an empty surface-state band of the $\sqrt{3} \times \sqrt{3}$-Ag substrate which have

Table 2
Comparisons among the proposed models for the $\sqrt{21} \times \sqrt{21}$ surface superstructure with Ag or Au adatoms, together with experimental and theoretical results

| Models | Adatoms | Adsorption site | Plane group | No. of Si-trimer atoms | |
|---|---|---|---|---|---|
| | | | | P component | Q component |
| Nogami et al. [1] | 5 Au | Ag triangle | p3 | 6 | 15 |
| Ichimiya et al. [2] | 3 Au | Si trimer | p3 | 12 | 9 |
| Tong et al. [6] | 4 Ag | Ag triangle | p1 | 9 | 12 |
| Tajiri et al. [19] | 5 Au | Ag triangle | p3 | 9 | 12 |
| Theory [14] | | Ag triangle | | | |
| Core-level PES[a] | | | | 12 | 9 |

[a] Present work.

maximum density-of-states at the centers of Ag triangles. Thus the adatoms are positively ionized.

In the initial-state picture of photoemission, the core-level shift towards lower binding energy of the Q component suggests that extra electrons exist at this sites of Si atoms. The extra electrons should originate from the Ag adatom sitting at the center of the nearby Ag triangles. Charge transfer occurs from the Ag adatom to the Ag triangle as revealed by the above-mentioned ARPES of valence bands, and then further transferred from the Ag-triangle atoms to the Si-trimer atoms due to a larger electronegativity of Si than that of Ag atoms.

The intensity ratio between the P and Q components is P:Q = 4:3, as shown in Table 1, which means that there are 12 'unaffected' Si atoms and 9 'affected' Si atoms in the unit cell. This result excludes the models of Nogami et al., Tong et al. and Tajiri et al. (see the last column in Table 2). The model of Ichimiya et al. only seems consistent to the measured intensity ratio. It is, however, already excluded by the theoretical calculations that Ag adatoms do not prefer to adsorb on the Si trimers [14]. As a result, none of the structure models proposed so far for the $\sqrt{21} \times \sqrt{21}$ phases satisfy the requirements from the experimental and theoretical results available. These requirements are listed in the last two rows in Table 2. Although we cannot propose a new model at the moment, these requirements should be considered seriously for the future structure analysis of the $\sqrt{21} \times \sqrt{21}$ surface superstructures.

## 5. Summary

We studied the Si 2p surface core-level shifts during a structure conversion from the Si(1 1 1)–$\sqrt{3} \times \sqrt{3}$-Ag into $\sqrt{21} \times \sqrt{21}$-Ag surfaces by adsorbing sub-monolayer Ag adatoms at 140 K. The $S_1$ component of the Si 2p emission from the Si-trimer atoms on the $\sqrt{3} \times \sqrt{3}$-Ag phase was found to split into two components P and Q on the $\sqrt{21} \times \sqrt{21}$-Ag phase, while another surface component $S_2$ hardly changed. The Q component with an energy shift towards lower binding energy was assigned to associate with the Si-trimer atoms that bond to Ag triangles with Ag adatoms sitting on ('affected' Si atoms), while the P component at nearly the same energy position as the initial $S_1$ component was assigned to the Si-trimer atoms that bond to Ag triangles without Ag adatoms sitting on ('unaffected' Si atoms). The intensity ratio between the P and Q components was useful to eliminate some of the structure models proposed so far. We found that there are no models that satisfy all the requirements from the experimental and theoretical results available.

## Acknowledgements

The present experiments were performed under the proposal number 98G035 of Photon Factory at KEK. This work has been supported in part by Grants-in-Aid from the Ministry of Education, Science, Culture, and Sports of Japan, especially through that for Creative Basic Research (No. 09NP1201). The CREST (Core Research for Evolutional Science and Technology) of the Japan Science and Technology Corporation (JST), and the Special Researcher of Basic Science Program in RIKEN are also acknowledged for the support.

## References

[1] J. Nogami, K.J. Wan, X.F. Lin, Surf. Sci. 306 (1994) 81.
[2] A. Ichimiya, H. Nomura, Y. Horio, Surf. Rev. Lett. 1 (1994) 1.
[3] Z.H. Zhang, S. Hasegawa, S. Ino, Phys. Rev. B 52 (1995) 10760.
[4] I. Homma, Y. Tanishiro, K. Yagi, in: S.Y. Tong, M.A. Van Hove, K. Takayanagi, X.D. Xie (Eds.), The Structure of Surfaces, Vol. III, Springer, Berlin, 1991, 610 pp.
[5] X. Tong, S. Hasegawa, S. Ino, Phys. Rev. B 55 (1997) 1310.
[6] X. Tong, Y. Sugiura, T. Nagao, T. Takami, S. Takeda, S. Ino, S. Hasegawa, Surf. Sci. 408 (1998) 146.
[7] S. Hasegawa, K. Tsuchie, K. Toriyama, X. Tong, T. Nagao, Appl. Surf. Sci. 162/163 (2000) 42.
[8] S. Hasegawa, X. Tong, S. Takeda, N. Sato, T. Nagao, Prog. Surf. Sci. 60 (1999) 89.
[9] M. Lijadi, H. Iwashige, A. Ichimiya, Surf. Sci. 357/358 (1996) 51.
[10] X. Tong, C.S. Jiang, S. Hasegawa, Phys. Rev. B 57 (1998) 9015.
[11] X. Tong, S. Ohuchi, N. Sato, T. Tanikawa, T. Nagao, I. Matsuda, Y. Aoyagi, S. Hasegawa, Phys. Rev. B 64 (2001) 205316.
[12] C.-S. Jiang, X. Tong, S. Hasegawa, S. Ino, Surf. Sci. 376 (1997) 69.
[13] S. Hasegawa, X. Tong, C.-S. Jiang, Y. Nakajima, T. Nagao, Surf. Sci. 386 (1997) 322.
[14] H. Aizawa, M. Tsukada, Phys. Rev. B 59 (1999) 10923.
[15] T. Takahashi, S. Nakatani, Surf. Sci. 283 (1993) 17 and references therein.
[16] G. LeLay, M. Gothelid, A. Cricenti, C. Hakansson, P. Perfetti, Europhys. Lett. 45 (1998) 65.
[17] Y. Nakajima, G. Uchida, T. Nagao, S. Hasegawa, Phys. Rev. B 54 (1996) 14134.
[18] G.S. Herman, J.C. Woicik, A.B. Andrews, J.L. Erskine, Surf. Sci. 290 (1993) L643.
[19] H. Tajiri, K. Sumitani, W. Yashiro, S. Nakatani, T. Takahashi, K. Akimoto, H. Sugiyama, X. Zhang, H. Kawata, Surf. Sci. 493 (2001) 214.